Atmos. Chem. Phys. Discuss., 11, 3857–3884, 2011
www.atmos-chem-phys-discuss.net/11/3857/2011/
doi:10.5194/acpd-11-3857-2011

Atmospheric Chemistry and Physics Discussions

Modelling the effect of denitrification on polar ozone depletion for Arctic winter/spring 2004/05

W. Feng[1,2], **M. P. Chipperfield**[1], **S. Davies**[1], **G. W. Mann**[1], **K. S. Carslaw**[1], **and S. Dhomse**[1]

[1]Institute for Climate and Atmospheric Science, School of Earth and Environment, University of Leeds, Leeds, UK
[2]Mathematics and Physical Sciences, School of Chemistry, University of Leeds, Woodhouse Lane, Leeds, LS2 9JT, UK

Received: 23 December 2010 – Accepted: 28 January 2011 – Published: 2 February 2011

Correspondence to: W. Feng (fengwh@env.leeds.ac.uk)

Published by Copernicus Publications on behalf of the European Geosciences Union.

Abstract

A three-dimensional (3-D) chemical transport model (CTM), SLIMCAT, has been used to quantify the effect of denitrification on ozone loss for the Arctic winter/spring 2004/05. The simulated HNO_3 is found to be highly sensitive to the polar stratospheric cloud (PSC) scheme used in the model. Here the standard SLIMCAT full chemistry model, which uses a thermodynamic equilibrium PSC scheme, overpredicts the Arctic ozone loss for Arctic winter/spring 2004/05 due to the overestimation of denitrification and stronger chlorine activation than observed. A model run with a detailed microphysical denitrification scheme, DLAPSE (Denitrification by Lagrangian Particle Sedimentation), is less denitrified than the standard model run and better reproduces the observed HNO_3 as measured by Airborne SUbmillimeter Radiometer (ASUR) and Aura Microwave Limb Sounder (MLS) instruments. The overestimated denitrification causes a small overestimation of Arctic polar ozone loss (~5–10% at ~17 km) by the standard model. Use of the DLAPSE scheme improves the simulation of Arctic ozone depletion compared with the inferred partial column ozone loss from ozonesondes and satellite data. Overall, denitrification is responsible for a ~30% enhancement in O_3 depletion for Arctic winter/spring 2004/05, suggesting that the successful simulation of the impact of denitrification on Arctic ozone depletion also requires the use of a detailed microphysical PSC scheme in the model.

1 Introduction

Significant progress has been made in understanding the processes controlling the observed polar stratospheric ozone depletion during the recent decades through measurements, laboratory work and modelling studies (e.g., Solomon, 1999; Chipperfield et al., 2005). Previous extensive studies have shown that successfully understanding polar stratospheric ozone depletion depends crucially on the processes of polar stratospheric clouds (PSCs) in activating chlorine and denitrifying the stratosphere (e.g.,

ACPD
11, 3857–3884, 2011

Tabazadeh et al., 2000; WMO, 2006). Although the main processes that lead to ozone depletion are generally well understood, there remain open questions such as the duration of chlorine activation and its dependence on the abundance of nitrogen oxides (Kühl et al., 2004).

Reactive nitrogen (NO_y) species play an important role in the chemistry of stratospheric O_3, both directly through rapid catalytic cycles involving NO_x and indirectly through their interaction with e.g. halogen species. As stratospheric halogen levels decline, the role of NO_y species may become more important. However, over the past few years there have been a number of updates to laboratory data related to NO_y chemistry. In addition, studies using 3-D chemical transport models have indicated problems in reproducing the observed abundance of NO_y and its partitioning into its components. Denitrification is defined as the permanent removal of NO_y from a stratospheric air mass by the sedimentation of HNO_3-containing particles (e.g., Fahey et al., 1990; Kleinböhl et al., 2005). Significant denitrification leads to an increase in the lifetime of ozone-depleting chlorine species (ClO_x) and therefore leads to an increase in the duration and extent of springtime polar ozone loss (e.g., Esler and Waugh, 2002; Davies et al., 2002).

The Arctic winter/spring 2004/05 was one of the coldest winters ever recorded in the stratosphere, and has been studied extensively (e.g., Manney et al., 2006; Rex et al., 2006; von Hobe et al., 2006; Feng et al., 2007a; Singleton et al., 2007; Rosevall et al., 2008). Feng et al. (2007a) found that a latest version of the SLIMCAT 3-D chemical transport model (CTM) (Chipperfield, 2006) overestimated the observed ozone loss in the cold Arctic winter/spring of 2004/05. Therefore, further investigations of the processes which lead to Arctic ozone depletion are required to better understand the discrepancies between models and observed ozone loss. Previously models had systematically underestimated Arctic ozone loss in cold winters (e.g., Becker et al., 1998; Rex et al., 2004; Feng et al., 2005a; Chipperfield et al., 2005 and Singleton et al., 2005). More details in the updated SLIMCAT can be found in (Feng et al., 2005a; Chipperfield et al., 2005; Chipperfield, 2006; Feng et al., 2007b; thereafter).

ACPD
11, 3857–3884, 2011

In this paper, we investigate the impact of using different model PSC schemes, including denitrification effect on the ozone loss for the Arctic winter/spring 2004/05. We use airborne and satellite remote sensing observations from the ASUR (Airborne SUbmillimeter Radiometer) and Aura MLS (Microwave Limb Sounder) instruments to test the denitrification simulated by the model for the different PSC schemes.

2 ASUR and Aura MLS measurements

The Airborne SUbmillimeter Radiometer (ASUR) (Küllmann et al., 1999) is an airborne radiometer measuring the thermal emission of trace gases in the stratosphere. The instrument was successfully operated on board the NASA DC-8 research aircraft in the Polar Aura Validation Experiment (PAVE) over the period of 24 January to 9 February 2005 remotely measuring the trace gases HCl, O_3, ClO, N_2O and HNO_3 in the altitude range 14 to 40 km (Kleinböhl et al., 2005; Kuttippurath et al., 2004).

The Earth Observing System (EOS) Microwave Limb Sounder (MLS) is an instrument on the NASA EOS Aura satellite, launched on 15 July 2004. It observes a large suite of atmospheric parameters by measuring millimetre and submillimetre wavelength thermal emission from the Earth's limb viewing forward along the Aura spacecraft flight track. Vertical profiles of O_3, HNO_3, ClO, HCl, N_2O, H_2O, CO and other chemical compounds are retrieved. Aura MLS has better spatial resolution and coverage than the older UARS MLS instrument with measurement made globally on daily basis. A feature of the MLS technique is that its measurements can be obtained in the presence of ice clouds and aerosol, that prevent measurements by shorter-wavelength infrared, visible and ultraviolet techniques (for more information see http://mls.jpl.nasa.gov or Livesey et al., 2006; Waters et al., 2006; Santee et al., 2007). The MLS data used in this paper is version 1.5 as described in Santee et al. (2008).

The ASUR and MLS data are very useful for understanding stratospheric ozone depletion and for validating atmospheric chemical transport models. Here we will concentrate on the chemical species HNO_3, HCl, ClO, O_3 and N_2O. The observations

ACPD
11, 3857–3884, 2011

of HNO_3 during the polar winter allow the quantification of denitrification. The chlorine compounds HCl and ClO permit a testing of chlorine activation and other related chemical processes. N_2O will be used to determine changes due to atmospheric dynamics in the polar region (i.e., diabatic descent of air masses in the atmosphere) and validate the model transport. O_3 data will be used to check the atmospheric dynamical and chemical processes.

3 Model and experiments

SLIMCAT is an off-line 3-D CTM described in detail by Chipperfield (1999, 2006) which now uses a hybrid σ-θ as vertical coordinate and includes the atmosphere from the surface up to ~60 km. The model has been widely used to study transport and chemistry in the upper troposphere and lower stratosphere (UTLS) (e.g., Feng et al., 2005a, b; Chipperfield, 2006; Feng, 2006; Feng et al., 2007a, b). Horizontal winds and temperatures are specified using meteorological analyses. Vertical advection is calculated from diabatic heating rates using a NCAR CCM radiation scheme (Briegleb, 1992) which gives a better representation of vertical transport in the model (see Feng et al., 2005a). Chemical tracers in SLIMCAT are advected using the scheme of Prather (1986) which conserves second-order moments and performs well in maintaining strong gradients. The model contains the principal stratospheric chemical species in the O_x, HO_x, NO_y, Cl_y, Br_y families as well as source gases (i.e., N_2O, CH_4, $CFCl_3$, CF_2Cl_2, CH_3Br) and a treatment of CH_4 oxidation. The photochemical data is based on the JPL recommendation (Sander et al., 2006) with the exception of the absorption cross sections of Cl_2O_2 which is taken from Burkholder et al. (1990) extrapolated to 450 nm. The Burkholder et al. (1990) cross-section (updated by Papanastasiou et al., 2009) are larger than other laboratory measurements, and have been found to reproduce the observed Arctic ozone loss rate (see SPARC, 2009). The model contains a detailed gas-phase stratospheric chemistry scheme and also a treatment of heterogeneous reactions on liquid aerosols, nitric acid trihydrate (NAT) and ice (see Chipperfield, 1999).

ACPD
11, 3857–3884, 2011

The standard SLIMCAT model uses a simplified PSC scheme for the determination of heterogeneous chemistry and denitrification, based on assuming thermodynamic equilibrium between the particles formed (whether liquid aerosol, NAT or ice) and the gas phase (e.g., Davies et al., 2002; Davies, 2003; Feng et al., 2005a, 2007a, b; Chipperfield et al., 2005). The equilibrium model assumes NAT forms in two modes (radii 0.5 and 6.5 µm), which is the same as the scheme described by Davies et al. (2002) and tested for the cold winter of 1999/2000 (Feng et al., 2005a). In this scheme NAT particles are sedimented from the model with fall velocities of 1 and 1100 m/day appropriate for particles of radius 0.5 and 6.5 µm, respectively. Ice particles with an assumed radius of 10 µm are sedimented at a rate of 1500 m/day.

However, a full microphysical PSC scheme is required for a detailed simulation of Arctic denitrification. Previous studies (e.g., Davies et al., 2002, 2006; Davies, 2003; Mann et al., 2002, 2003, 2005) used the separate microphysical model DLAPSE (Denitrification by Lagrangian Particle Sedimentation) to investigate denitrification effect in Arctic winters, but only Davies et al. (2006) combined this with the full SLIMCAT chemistry. These studies advected gas phase HNO_3 in SLIMCAT, interpolated to the Lagrangian particle positions, then ran the DLAPSE model to calculate the growth and sedimentation of several hundred thousand particles (more details can be found in Davies, 2003). In Davies et al. (2006), they were running two independent models (DLAPSE and SLIMCAT) and passing information between these two models. For this work, we have fully incorporated the Lagrangian particle denitrification model (DLAPSE) into the SLIMCAT model to extend the options of PSC scheme in the model. The coupled DLAPSE model uses the Lagrangian trajectory scheme contained in the SLIMCAT model (see Monge-Sanz et al., 2007). This is an improvement over the standard model because it calculates the growth and sedimentation of individual particles and is suitable for the simultaneous simulation of several hundred thousand particles (Carslaw et al., 2002). Despite the microphysical detail, the coupled DLAPSE model is computationally efficient as it only performs calculations when NAT particles are present and does not add any additional 3-D tracers in the model.

ACPD
11, 3857–3884, 2011

Three model experiments with different treatment of PSCs were run for the Arctic winter/spring of 2004/05 (Table 1). Experiment A (EXP_A) is the standard SLIMCAT full chemistry run as described in Feng et al. (2007a), Experiment B (EXP_B) is the full chemistry run using the microphysical DLAPSE scheme. Here we used a constant volume average NAT nucleation rate (8.1×10^{-10} particles cm^{-3} s^{-1}). NAT particles are initialised with a radius of 0.1 µm. Finally, Experiment C (EXP_C) had denitrification switched off (no sedimentation). All of these model experiments used 24 vertical levels extending from the surface to ~60 km and a horizontal resolution of 2.8° × 2.8°. The model was forced by 6-hourly European Centre for Medium-Range Weather Forecasts (ECMWF) operational analyses.

4 Results

Figure 1 shows profiles of HNO_3, HCl, O_3 and N_2O from ASUR, MLS and the three SLIMCAT simulations for 31 January 2005. Figure 2 is similar to Fig. 1 but for 5 February 2005 (here MLS data is not shown; the quality of MLS data near this location on this day needs further investigation). Kleinböhl et al. (2005) noted that flights on these two days penetrated deep into the vortex. The observed HNO_3 decreases with altitude from ~13 to ~22 km, increases with altitude to ~26 km and then decreases again in the middle and upper stratosphere, which is indicative of significant denitrification having occurred. MLS HNO_3 has a very similar profile below 16 km and above 25 km with ASUR. However, there is a large bias between 18–24 km (not shown), possibly due to an error in one of the spectroscopy files used in MLS version 1.5 processing (M. Santee, personal communication, 2010). Overall, the model simulation EXP_A captures the observed profile well, but some differences exist. For example, EXP_A underestimates HNO_3 at 14 km (2–3 ppbv) and overestimates it around 25 km. By contrast, EXP_B using the microphysics DLAPSE denitrification scheme captures the profile remarkably well. The model with the thermodynamic equilibrium PSC scheme overestimates denitrification of the lower stratosphere, while the simulation using the

ACPD
11, 3857–3884, 2011

more detailed microphysical denitrification scheme is in excellent agreement with observed HNO_3 from ASUR measurements from 15 to 20 km, where the PSCs dominate and play important role in denitrification.

The ASUR measurements detected evidence for Cl activation from the absence of HCl between 16 and 22 km on the flights of 31 January and 5 February (the negative ASUR HCl values at 18 and 20 km are not shown here). The vertical distribution of HCl in the full chemical model compares fairly well to ASUR if denitrification is included. However, the model compares better with HCl at higher altitudes if denitrification is not included in the model EXP_C, suggesting that SLIMCAT with full chemistry and denitrification greatly overestimated chlorine activation at ~22 km for the latter part of the Arctic winter/spring 2004/05. This result is also confirmed when the modelled HCl is compared with MLS data (see also Santee et al., 2008). The modelled ozone values in the lower stratosphere at 16–18 km are very close to the MLS and ASUR data. However, the model underestimates ASUR observed O_3 above 28 km but this is not the relevant region for polar stratospheric ozone depletion and agreement with MLS is better. There is still some O_3 difference between EXP_A and EXP_C (though it is small) at ~17 km due to the effect of denitrification on O_3 loss at this time of the year. Profiles of the long-lived species N_2O can be used to verify modelled tracer transport (Feng et al., 2005a). The model has too strong descent in the lower stratosphere when compared with MLS and ASUR data for the flight on 31 January and also for the flight on 5 February.

Figure 3 shows the relative difference of profiles of HNO_3, HCl and O_3 from ASUR, model simulations using two different PSC schemes (EXP_A, EXP_B) and the model run without denitrification (EXP_C) for 31 January and 5 February 2005. Again, the SLIMCAT simulation using the thermodynamic equilibrium has larger denitrification (relative difference is about 50–70% at 16–20 km) than using the microphysical DLAPSE scheme (~50–60%) which is comparable with the relative difference between ASUR and EXP_C (~50%). The modelled HCl from EXP_B also has a similar difference (~50%) between ASUR and EXP_C in the lower stratosphere in particular for 31

ACPD
11, 3857–3884, 2011

January 2005. The relative O_3 differences between EXP_A, EXP_B and EXP_C are quite small (less than 10%) though there are larger relative percent differences with observations.

Figure 4 shows the time series of averaged HNO_3, HCl, ClO, N_2O and O_3 inside the vortex on the 456 K isentropic level (~17 km) from MLS measurements and SLIMCAT simulations using the two PSC schemes (EXP_A and EXP_B) and no denitrification (EXP_C). Here the vortex is defined as the area enclosed by the 65° N equivalent latitude (EL) contour. Again, EXP_B, the SLIMCAT simulation with the detailed DLAPSE denitrification scheme, gives excellent agreement with observed HNO_3, where the equilibrium scheme overpredicts denitrification at 456 K. The model captures the temporal evolution of observed HCl and ClO, though the model with full chemistry again seems to have too much chlorine activation, resulting in overestimation of observed ozone loss (Feng et al., 2007a). The observed N_2O values inside the vortex decreased rapidly in early December, increased in late December, then decreased again until mid January. The model captures many features of observed N_2O evolution, but overall, model has more diabatic descent than MLS observations. Note that substantial improvement in the N_2O data has been achieved in MLS v2, with the elimination of a significant low bias in the stratosphere and correction of occasional unrealistically high mixing ratios in the polar regions (M. Santee, personal communication, 2010). Even though the modelled HNO_3 field is significantly improved when using the DLAPSE microphysical scheme (EXP_B), there is not much difference (less than 0.2 ppmv) in the simulated O_3 from the SLIMCAT full chemistry experiments (EXP_A and EXP_B) possibly because the same surface area of the liquid aerosol are used for the chlorine activation in these two experiments (EXP_A and EXP_B). This requires further detailed investigation. Obviously, the modelled ozone overestimates the observations if denitrification is not considered in the model (EXP_C).

Figure 5 shows the vortex-averaged modelled NO_y and ClO_x (= Cl + ClO + 2 × Cl_2O_2) as a function of time and potential temperature for Arctic winter/spring 2004/05 from the three simulations. The NO_y has values larger than 10 ppbv above 450 K in early

ACPD
11, 3857–3884, 2011

December but these decrease rapidly after mid December. Denitrification is predicted to have started in December and the very low ambient temperatures produce lower NO_y values due to PSC formation and denitrification between 400 and 530 K (~14 to 22 km). NO_y in EXP_A, using the thermodynamic equilibrium scheme, is as low as 3 ppbv by late January, indicating that extensive denitrification has occurred. As shown in Mann et al. (2002, 2003) when the cold pool is offset from the centre of rotation of the vortex, denitrification is weak due to short particle lifetimes. EXP_B, using DLAPSE scheme, captures this behaviour, but the standard SLIMCAT model based on the equilibrium scheme continues to predict denitrification.

Chlorine activation on PSCs occurred at high altitudes from early December and activation gradually extended downwards even to the lowermost stratosphere (below 400 K) which consistent with corresponding low temperatures and descent of air and potential PSC extent. Maximum ClO_x exceeded 2.7 ppbv from late December until early February. Modelled chlorine activation is reduced if denitrification is not considered in the model (EXP_C) as chlorine deactivation mainly occurs by the reaction of $ClO + NO_2 + M \rightarrow ClONO_2 + M$ and the time for stratospheric chlorine deactivation depends on the degree of denitrification. If NO_2 decreases due to the removal of nitrogen reservoirs by denitrification process, chlorine deactivation will be delayed. EXP_A using the equilibrium PSC scheme has stronger denitrification than EXP_B and has a longer deactivation time and prolonged Arctic ozone loss. The deactivation is even faster if no denitrification is included in the model. The DLAPSE denitrification scheme (EXP_B) has realistic denitrification, therefore, slowing down chemical ozone depletion compared to the thermodynamical equilibrium scheme (EXP_A).

Figure 6 is the absolute difference of vortex averaged modelled NO_y and ClO_x between the full chemistry simulations (EXP_A, EXP_B) and the SLIMCAT simulation without denitrification (EXP_C). Overall, the patterns of NO_y and ClO_x differences are very similar. Again, more extensive denitrification has occurred in the model with the thermodynamic equilibrium scheme (EXP_A) than with a detailed microphysical denitrification scheme DLAPSE (EXP_B). There are large ClO_x differences above 500 K (~21 km)

ACPD
11, 3857–3884, 2011

before mid-February and in the lower stratosphere in late February/early March. However, the difference in ClO_x is still small between EXP_A and EXP_B.

The ozone loss for Arctic winter/spring 2004/05 has been estimated through various methods by researchers using different measurements and/or models (e.g., Manney et al., 2006; Jin et al., 2006; Rex et al., 2006; Von Hobe et al., 2006; Singleton et al., 2007; Grooß and Müller, 2007; Feng et al., 2007a; Rösevall et al., 2008; Jackson and Orsolini, 2008). However, there are still large differences in the inferred maximum ozone loss (for details see Table 2). For Arctic winter/spring 2004/05, the ozone loss inferred from Odin satellite SMR (Sub-Millimetre Radiometer) is 0.6–1.3 ppmv (Rösevall et al., 2008), which is lower than from other measurements, while the inferred ozone loss from M55 Geophysica aircraft data and ACE-FTS (Atmospheric Chemistry Experiment-Fourier Transform Spectrometer) is higher (2.1–2.3 ppmv) (Von Hobe et al., 2006; Jin et al., 2006). The calculated ozone loss is 0.7–1.2 ppmv from the assimilation of measurements data into the models (Jackson and Orsolini, 2008; Rösevall et al., 2008). Singleton et al. (2007) estimated 2.0–2.3 ppmv ozone loss using data from different satellite instruments and the SLIMCAT model which is similar as Feng et al. (2007a). The calculated ozone loss is 1.08–1.66 ppmv from the 3-D CTM CLaMS (Chemical Lagrangian Model of the Stratosphere) (Grooß and Müller, 2007). The full chemistry of SLIMCAT with the simple thermodynamical equilibrium PSC scheme gives 2–2.3 ppmv ozone loss while it is slightly lower when used DLAPSE denitrification scheme. Clearly, SLIMCAT without denitrification has less ozone loss (0.6–0.8 ppmv) as expected.

Figure 7 shows time series of vortex-averaged ozone loss and maximum local ozone loss at 456 K and partial column ozone loss (380–550 K) from the three simulations (EXP_A, EXP_B and EXP_C). Arctic polar ozone depletion began in December in the cold polar vortex and strong chlorine activation regions and the maximum ozone loss was reached in mid March 2005, following by a decrease due to the vortex break-up and increased temperatures. The three simulations have a similar ozone loss signal, but using the equilibrium scheme (EXP_A) has slightly higher ozone loss than EXP_B, while the ozone loss is much less for EXP_C, when denitrification is switched off. The

ACPD
11, 3857–3884, 2011

lower stratospheric partial column ozone losses show very similar patterns. There is ~90 DU partial column ozone loss from the model without denitrification, much lower than the observed 121 ± 20 DU by Rex et al. (2006). The diagnosed partial column ozone loss from the model with the full microphysical DLAPSE scheme (EXP_B) is about 120 DU which better matches the observations (Rex et al., 2006), while the standard model based on a simple thermodynamic equilibrium PSC scheme slightly overestimates the observations. This clearly shows the importance of considering denitrification in the model and emphasises the sensitivity of Arctic ozone loss due to denitrification processes.

Figure 8 shows time series of differences in vortex-averaged ozone loss at 456 K and partial column ozone loss (380–550 K) between model sensitivity experiments (EXP_B, EXP_C) and standard SLIMCAT simulation (EXP_A) for Arctic winter/spring 2004/05. There are less ozone loss using a full microphysical DLAPSE denitrification scheme than using a simple thermodynamic equlibrium PSC scheme in SLIMCAT. The vortex averaged ozone loss is small (less than 0.2 ppmv) between the full chemistry SLIMCAT (EXP_B and EXP_A), The partial column ozone difference is ~10 DU in late winter/early spring 2004/05. However, there are larger ozone loss differences (1.2–1.6 ppmv at 456 K, 40–60 DU partial column ozone loss between 380–550 K) if denitrification is not considered in the model. This again emphases the importance of dentrification process for the Arctic ozone depletion.

5 Conclusions

We have used a three-dimensional (3-D) chemical transport model SLIMCAT to quantify the effect of denitrification on ozone loss for the Arctic winter/spring 2004/05. This is an extension work from Feng et al. (2007a). The standard SLIMCAT full chemistry model, when using a thermodynamic equilibrium PSC scheme, overestimates Arctic ozone loss for winter/spring 2004/05 due to too strong chlorine activation and the overestimation of denitrification. The model simulation using the microphysical

ACPD
11, 3857–3884, 2011

denitrification scheme DLAPSE successfully reproduces the observed HNO_3 as measured by the ASUR and Aura MLS instruments. The simulation from the model run without denitrification process underestimates the Arctic polar ozone depletion by ~30%, i.e. 40–60 DU partial column ozone loss for Arctic winter/spring 2004/05. The time taken for stratospheric chlorine deactivation depends crucially on the degree of denitrification. Therefore, accurately simulating the impact of denitrification on Arctic ozone depletion requires a detailed microphysical PSC scheme in the model. The simulations are quite sensitive to the PSC schemes used in the model, with a small (~5–10% at ~17 km) effect on Arctic ozone loss when using the simple equilibrium or the microphysical PSC scheme.

Atmospheric chemistry models, i.e., chemistry climate models (CCMs) and chemical transport models (CTMs), are now widely used to predict future stratospheric ozone change. However, most CCMs and CTMs are still using a simple thermodynamic equilibrium PSC schemes for the determination of heterogeneous chemistry and denitrification (e.g., SPARC CCMval, 2010). Many studies have shown that an increased severity of denitrification may delay the recovery of polar ozone in spring. Therefore, it would be very important to consider a full microphysical denitrification process in CCMs and CTMs for better simulations or predictions of current/future polar ozone trends in both hemispheres.

Acknowledgements. This work was supported by the EU SCOUT-O3 and UK Natural Environment Research Council (NERC). The MLS data was provided by Lynn Harvey at Laboratory for Atmospheric and Space Physics, University of Colorado. We would like to thank with Michelle Santee for discussions. The ECMWF analyses were obtained via the British Atmospheric Data Centre.

References

Briegleb, B. P.: Delta-Eddington approximation for solar radiation in the NCAR community climate model, J. Geophys. Res., 97, 7603–7612, 1992.

ACPD
11, 3857–3884, 2011

Becker, G., Müller, R., Mckenna, D. S., Rex, M. and Carslaw, K. S.: Ozone loss rates in the Arctic stratosphere in the winter 1991/92: Model calculations compared with match results, Geophys. Res. Lett., 25, 4325–4328, doi:10.1029/1998GL900148, 1998.

Burkholder, J. B., Orlando, J. J., and Howard, C. J.: Ultraviolet-absorption cross-sections of Cl_2O_2 between 210 and 410 nm, J. Phys. Chem., 94, 687–695, 1990.

Carslaw, K. S., Kettleborough, J. A., Northway, M. J., Davies, S., Gao, R. S., Fahey, D. W., Baumgardner, D. G., Chipperfield, M. P., and Kleinböhl, A.: A vortex-scale simulation of the growth and sedimentation of large nitric acid hydrate particles, J. Geophys. Res., 107, 8300, doi:10.1029/2001JD000467, 2002.

Chipperfield, M. P.: Multiannual simulations with a three-dimensional chemical transport model, J. Geophys. Res., 104, 1781–1805, 1999.

Chipperfield, M. P.: New version of the TOMCAT/SLIMCAT off-line chemical transport model: Intercomparison of stratospheric tracer experiments, Q. J. Roy. Meteorol. Soc., 132, 1179–1203, doi:10.1256/qj.05.51, 2006.

Chipperfield, M. P., Feng, W., and Rex, M.: Arctic ozone loss and climate sensitivity: Updated three-dimensional model study, Geophys. Res. Lett., 32, L11813, doi:10.1029/2005GL022674, 2005.

Davies, S.: Denitrification and ozone loss in the Arctic stratosphere, PhD dissertation, University of Leeds, 191 pp., 2003.

Davies, S., Chipperfield, M. P., Carslaw, K. S., Sinnhuber, B.-M., Anderson, J. G., Stimpfle, R. M., Wilmouth, D. M., Fahey, D. W., Popp, P. J., Richard, E. C., von der Gathen, P., Jost, H., and Webster, C. R.: Modeling the effect of denitrification on Arctic ozone depletion during winter 1999/2000, J. Geophys. Res., 107, 8322, doi:10.1029/2001JD000445, 2002.

Davies, S., Mann, G. W., Carslaw, K. S., Chipperfield, M. P., Remedios, J. J., Allen, G., Waterfall, A. M., Spang, R., and Toon, G. C.: Testing our understanding of Arctic denitrification using MIPAS-E satellite measurements in winter 2002/2003, Atmos. Chem. Phys., 6, 3149–3161, doi:10.5194/acp-6-3149-2006, 2006.

Esler, J. G. and Waugh, D. W.: A method for estimating the extent of denitrification of Arctic polar vortex air from tracer-tracer scatter plots, J. Geophys. Res., 107, 4169,, doi:10.1029/2001JD001071, 2002.

Fahey, D. W., Solomon, S., Kawa, S. R., Loewenstein, M., Podolske, J. R., Strahan, S. E., and Chan, K. R.: A diagnostic for denitrification in the winter polar stratospheres, Nature, 345, 698–702, 1990.

ACPD
11, 3857–3884, 2011

Feng, W.: Fast ozone loss around the polar vortex during 2002/2003 Arctic winter deep minihole event, Water Air Soil Pollut., 171, 383–397, 2006.
Feng, W., Chipperfield, M. P., Davies, S., Sen, B., Toon, G., Blavier, J. F., Webster, C. R., Volk, C. M., Ulanovsky, A., Ravegnani, F., von der Gathen, P., Jost, H., Richard, E. C., and Claude, H.: Three-dimensional model study of the Arctic ozone loss in 2002/2003 and comparison with 1999/2000 and 2003/2004, Atmos. Chem. Phys., 5, 139–152, doi:10.5194/acp-5-139-2005, 2005a.
Feng, W., Chipperfield, M. P., Roscoe, H. K., Remedios, J. J., Waterfall, A. M., Stiller, G. P., Glatthor, N., Hopfner, M., and Wang, D.-Y.: Three-dimensional model study of the Antarctic ozone hole in 2002 and comparison with 2000, J. Atmos. Sci., 62, 822–837, 2005b.
Feng, W., Chipperfield, M. P., Davies, S., von der Gathen, P., Kyrö, E., Volk, C. M., Ulanovsky, A., and Belyaev, G.: Large chemical ozone loss in 2004/2005 Arctic winter/spring, Geophys. Res. Lett., 34, L09803, doi:10.1029/2006GL029098, 2007a.
Feng, W., Chipperfield, M. P., Dorf, M., Pfeilsticker, K., and Ricaud, P.: Mid-latitude ozone changes: studies with a 3-D CTM forced by ERA-40 analyses, Atmos. Chem. Phys., 7, 2357–2369, doi:10.5194/acp-7-2357-2007, 2007b.
Grooß, J.-U. and Müller, R.: Simulation of ozone loss in Arctic winter 2004/2005, Geophys. Res. Lett., 34, L05804, doi:10.1029/2006GL028901, 2007.
Jackson, D. R. and Orsolini, Y. J.: Estimation of Arctic ozone loss in winter 2004/05 based on assimilation of EOS MLS and SBUV/2 observations, Q. J. Roy. Meteorol. Soc., 134, 1833–1841, 2008.
Jin, J. J., Semeniuk, K., Manney, G. L., Jonsson, A. I., Beagley, S. R., McConnell, J. C., Dufour, G., Nassar, R., Boone, C. E., Walker, K. A., Bernath, P. F., and Rinsland, C. P.: Severe Arctic ozone loss in the winter 2004/2005: Observations from ACE-FTS, Geophys. Res. Lett., 33, L15801, doi:10.1029/2006GL026752, 2006.
Kleinböhl A., Bremer, H., Küllmann, H., Kuttippurath, J., Browell, E. V., Canty, T., Salawitch, R. J., Toon, G. C., and Notholt, J.: Denitrification in the Arctic mid-winter 2004/2005 observed by Airborne SUbmillimeter Radiometry, Geophys. Res. Lett., 32, L19811, doi:10.1029/2005GL023408, 2005.
Kühl, S., Wilms-Grabe, W., Beirle, S., Frankenberg, C., Grzegorski, M., Hollwedel, J., Khokhar, F., Kraus, S., Platt, U., Sanghavi, S., von Friedeburg, C., and Wagner, T.: Stratospheric chlorine activation in the Arctic winters 1995/96–2001/02 derived from GOME OClO measurements, Adv. Space Res., 34, 798–803, 2004.

ACPD
11, 3857–3884, 2011

Küllmann, H., Bremer, H., König, M., Künzi, K., Goede, A. R. W., Kleipool, Q. L., and Hetzheim, H.: The ASUR Sensor: A state-of the art remote sensing instrument for stratospheric trace gas measurements, Air pollution research report 73, Proceedings Fifth European Symposium on Stratospheric Ozone, 699–702, 1999.

Kuttippurath, J., Kleinböhl, A., Bremer, H., Küllmann, H., Von Savigny, C., and Notholt, J.: Validation of SCIAMACHY ozone limb profiles by ASUR, Proceedings of the second workshop on the atmospheric chemistry validation of ENVISAT(ACVE-2), ESA-ESRIN, Frascati, Italy, 3–7 May 2004, 2004.

Livesey, N. J., Synder, W. V., Read, W. G., and Wagner, P. A.: Retrieval algorithms for the EOS Microwave Limb Sounder (MLS), IEEE T. Geosci. Remote, 44, 1144–1155, 2006.

Mann G. W., Davies, S., Carslaw, K. S., Chipperfield, M. P., and Kettleborough, J.: Polar vortex concentricity as a controlling factor in Arctic denitrification, J. Geophys. Res., 107, 4663, doi:10.1029/2002JD002102, 2002.

Mann, G. W., Davies, S., Carslaw, K. S., and Chipperfield, M. P.: Factors controlling Arctic denitrification in cold winters of the 1990s, Atmos. Chem. Phys., 3, 403–416, doi:10.5194/acp-3-403-2003, 2003.

Mann G. W., Carslaw, K. S., Chipperfield, M. P., Davies, S., and Eckermann, S. D.: Large nitric acid trihydrate particles and denitrification caused by mountain waves in the Arctic stratosphere, J. Geophys. Res., 110, D08202, doi:10.1029/2004JD005271, 2005.

Manney, G. L., Santee, M. L., Froidevaux, L., Hoppel, K., Livesey, N. J., and Waters, J. W., EOS MLS observations of ozone loss in the 2004-2005 Arctic winter, Geophys. Res. Lett., 33, L04802, doi:10.1029/2005GL024494, 2006.

Monge-Sanz, B., Chipperfield, M. P., Simmons, A., and Uppal, S.: Mean age of air and transport in a CTM: Comparison of different ECMWF analyses, Geophys. Res. Lett., 34, L04801, doi:10.1029/2006GL028515, 2007.

Papanastasiou, D. K., Papadimitriou, V. C., Fahey, D. W., and Burkholder, J. B.: UV absorption spectrum of the ClO dimer (Cl_2O_2) between 200 and 420 nm, J. Phys. Chem., 113, 13711–13726, doi:10.1021/jp9065345, 2009.

Prather, M. J.: Numerical advection by conservation of second-order moments, J. Geophys. Res., 91, 6671–6681, 1986.

Rex, M., Salawitch, R. J., von der Gathen, P., Harris, N. R. P., Chipperfield, M. P., and Naujokat, B.: Arctic ozone loss and climate change, Geophys. Res. Lett., 31, L04116, doi:10.1029/2003GL018844, 2004.

ACPD
11, 3857–3884, 2011

Rex, M., Salawitch, R. J., Deckelmann, H., von der Gathen, P., Harris, N. R.P., Chipperfield, M. P., Naujokat, B., Reimer, E., Allaart, M., Andersen, S. B., Bevilacqua, R., Braathen, G. O., Claude, H., Davies, J., De Backer, H., Dier, H., Dorokhov, V., Fast, H., Gerding, M., Godin-Beekmann, S., Hoppel, K., Johnson, B., Kyrö, E., Litynska, Z., Moore, D., Nakane, H., Parrondo, M. C., Risley, A. D., Skrivankova, P., Stübi, R., Viatte, P., Yushkov, V., and Zerefos, C.: Arctic winter 2005: Implications for stratospheric ozone loss and climate change, Geophys. Res. Lett., 33, L23808, doi:10.1029/2006GL026731, 2006.

Rösevall, J., Murtagh, D. P., Urban, J., Feng, W., Eriksson, P., and Brohede, S.: A study of ozone depletion in the 2004/2005 Arctic winter based on data from Odin/SMR and Aura/MLS, J. Geophys. Res., 113, D13301, doi:10.1029/2007JD009560, 2008.

SPARC, Stratospheric Processes and Their Role in Climate: The Role of Halogen Chemistry in Polar Stratospheric Ozone Depletion: Report from the June 2008 Cambridge, UK Workshop for an Initiative under the Stratospheric Processes and Their Role in Climate (SPARC) Project of the World Climate Research Programme, available at: http://www.atmosp.physics.utoronto.ca/SPARC/HalogenChem_Final_20090213.pdf, edited by: Kurylo, M. J. and Sinnhuber, B.-M., 48 pp., 2009.

Sander, S. P., Ravishankara, A. R., Friedl, R. R., Golden, D. M., Kolb, C. E., Kurylo, M. J., Molina, M. J., Huie, R. E., Orkin, V. L., Moortgat, G. K., and Finlayson-Pitts, B. J.: Chemical kinetics and photochemical data for use in stratospheric modeling, Update to Evaluation no. 14, JPL Publ., 02-25, 2006.

Santee, M. L., Lambert, A., Read, W. G., Livesey, N. J., Cofield, R. E., Cuddy, D. Y., Daffer, W. H., Drouin, B. J., Froidevaux, L., Fuller, R. A., Jarnot, R. F., Knosp, B. W., Manney, G. L., Perun, V. S., Snyder, W. V., Stek, P. C., Thurstans, R. P., Wagner, P. A., Waters, J. W., Muscari, G., de Zafra, R. L., Dibb, J. E., Fahey, D. W., Popp, P. J., Marcy, T. P., Jucks, K. W., Toon, G. C., Stachnik, R. A., Bernath, P. F., Boone, C. D., Walker, K. A., Urban, J., and Murtagh, D.: Validation of Aura Microwave Limb Sounder HNO_3 measurements, J. Geophys. Res., 112, D24S40, doi:10.1029/2007JD008721, 2007.

Santee, M. L., MacKenzie, I. A., Manney, G. L., Chipperfield, M. P., Bernath, P. F., Walker, K. A., Boone, C. D., Froidevaux, L., Livesey, N. J., and Waters, J. W.: A study of stratospheric chlorine partitioning based on new satellite measurements and modeling, J. Geophys. Res., 113, D12307, doi:10.1029/2007JD009057, 2008.

Singleton, C. S., Randall, C. E., Chipperfield, M. P., Davies, S., Feng, W., Bevilacqua, R. M., Hoppel, K. W., Fromm, M. D., Manney, G. L., and Harvey, V. L.: 2002–2003 Arctic ozone loss

ACPD
11, 3857–3884, 2011

deduced from POAM III satellite observations and the SLIMCAT chemical transport model, Atmos. Chem. Phys., 5, 597–609, doi:10.5194/acp-5-597-2005, 2005.

Singleton, C. S., Randall, C. E., Harvey, V. L., Chipperfield, M. P., Feng, W., Manney, G. L., Froidevaux, L., Boone, C. D., Bernath, P. F., Walker, K. A., McElroy, C. T., and Joppel, K. W.: Quantifying Arctic ozone loss during the 2004–2005 winter using satellite observations and a chemical transport model, J. Geophys. Res., 112, D07304, doi:10.1029/2006JD007463, 2007.

Solomon, S.: Stratospheric ozone depletion: A review of concepts and history, Rev. Geophys., 37, 275–316, 1999.

SPARC CCMVal: SPARC Report on the Evaluation of Chemistry-Climate Models, edited by: Eyring, V., T.G. Shepherd, D.W. Waugh, SPARC Report No. 5, WCRP-132, WMO/TD-No. 1526, 2010.

Tabazadeh, A., Santee, M. L., Danilin, M. Y., Pumphrey, H. C., Newman, P. A., Hamill, P. J., and Mergenthaler, J. L.: Quantifying denitrification and its effect on ozone recovery, Science, 288, 1407–1411, 2000.

von Hobe, M., Ulanovsky, A., Volk, C. M., Grooß, J.-U., Tilmes, S., Konopka, P., Günther, G., Werner, A., Spelten, N., Shur, G., Yushkov, V., Ravegnani, F., Schiller, C., Müller, R., and Stroh, F.: Severe ozone depletion in the cold Arctic winter 2004–05, Geophys. Res. Lett., 33, doi:10.1029/2006GL026945, 2006.

Waters, J. W., Froidevaux, L., Harwood, R. S., Jarnot, R. F., Pickett, H. M., Read, W. G., Siegel, P. H., Cofield, R. E., Filipiak, M. J., Flower, D. A., Holden, J. R., Lau, G. K., Livesey, N. J., Manney, G. L., Pumphrey, H. C., Santee, M. L., Wu, D. L., Cuddy, D. T., Lay, R. R., Loo, M. S., Perun, V. S., Schwartz, M. J., Stek, P. C., Thurstans, R. P., Boyles, M. A., Chandra, K. M., Chavez, M. C., Chen, G. S., Chudasama, M. V., Dodge, R., Fuller, R. A., Girard, M. A., Jiang, J. J., Jiang, Y., Knosp, B. W., LaBelle, R. C., Lam, J. C., Lee, K. A., Miller, D., Oswlad, J. E., Patel, N. C., Pukala, D. M., Quintero, O., Scaff, D. M., Van Synder, W., Tope, M. C., Wagner, P. A., and Walch, M. J.: The Earth Observing System Microwave Limb Sounder (EOS MLS) on the Aura satellite, IEEE T. Geosci. Remote, 44, 1075–1092, 2006.

WMO (World Meteorological Organization): Scientific assessment of ozone depletion: 2006. Global Ozone Res. Monit. Proj. No., 50, Geneva, Switzerland, 572 pp., 2007.

ACPD
11, 3857–3884, 2011

Table 1. SLIMCAT model experiments.

Runs	Denitrification scheme	Reference
EXP_A	Thermodynamical equilibrium	Feng et al. (2007a)
EXP_B	Microphysical DLAPSE	Davies et al. (2006)
EXP_C	None	

ACPD
11, 3857–3884, 2011

Table 2. Inferred maximum ozone loss for Arctic winter/spring 2004/05

Reference	*Model*/Measurement	Ozone loss
Manney et al. (2006)	EOS MLS	1.2–1.5 ppmv (vortex) 2 ppmv (vortex edge)
Rösevall et al. (2008)	Aura MLS	0.9–1.3 ppmv
Rösevall et al. (2008)	Odin SMR	0.6–1.3 ppmv
Jin et al. (2006)	ACE-FTS	2.1 ppmv
Rex et al. (2006)	Ozonesondes/SAGE III/POAM III	1.2–1.8 ppmv
Von Hobe et al. (2006)	M55 Geophysica aircraft	2.1–2.3 ppmv
Rösevall et al. (2008)	*DIAMOND*+Odin SMR	*1.0–1.1* ppmv
Rösevall et al. (2008)	*DIAMOND*+Aura MLS	*0.7–0.9* ppmv
Jackson and Orsolini (2008)	*Met Office*+EOS MLS/SBUV	*0.8–1.2* ppmv
Singleton et al. (2007)	*SLIMCAT*/EOS MLS/POAM III /SAGE III/ACE-FTS/MAESTRO	*2–2.3* ppmv
Grooß and Müller (2007)	*CLaMS*	*1.08–1.66* ppmv
Feng et al. (2007a)	*SLIMCAT*:EXP_A	*2–2.3* ppmv
This work	*SLIMCAT*:EXP_B	*2–2.13* ppmv
This work	*SLIMCAT*:EXP_C	*0.6–0.8* ppmv

ACPD
11, 3857–3884, 2011

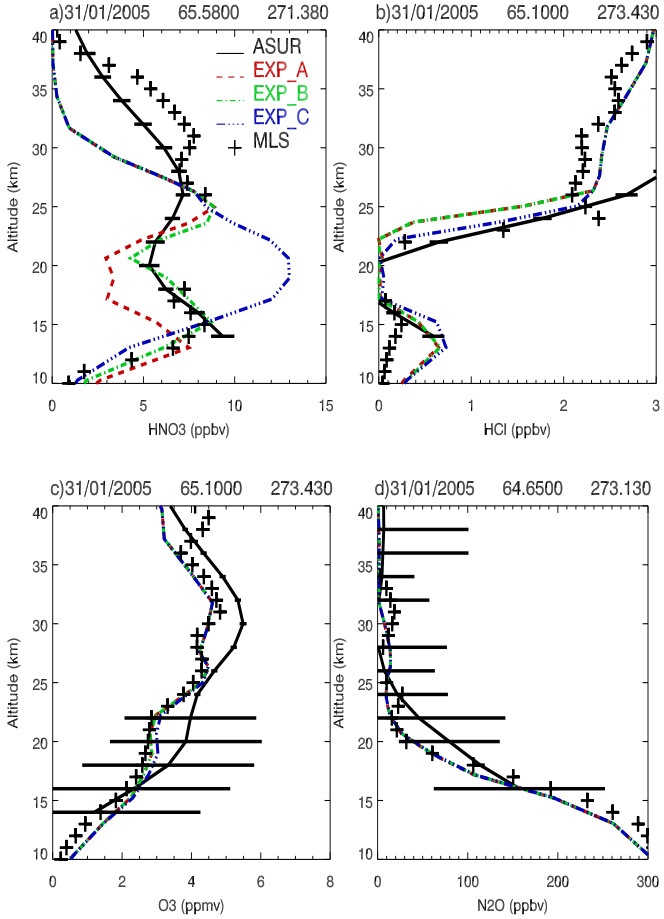

Fig. 1. HNO_3, HCl, O_3 and N_2O profiles from ASUR and MLS observations and model simulations using the equilibrium (EXP_A), DLAPSE (EXP_B) PSC schemes and without denitrification (EXP_C) for 31 January 2005.

ACPD
11, 3857–3884, 2011

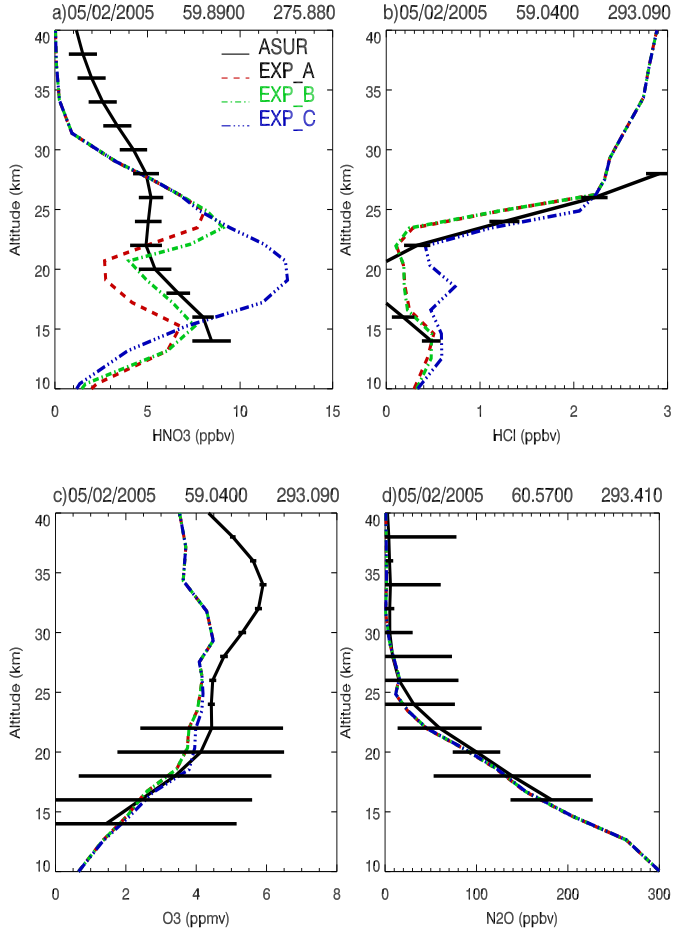

Fig. 2. HNO_3, HCl, O_3 and N_2O from ASUR observations and model simulations using equilibrium (EXP_A), DLAPSE(EXP_B) PSC schemes and without denitrification (EXP_C) for 5 February 2005.

ACPD
11, 3857–3884, 2011

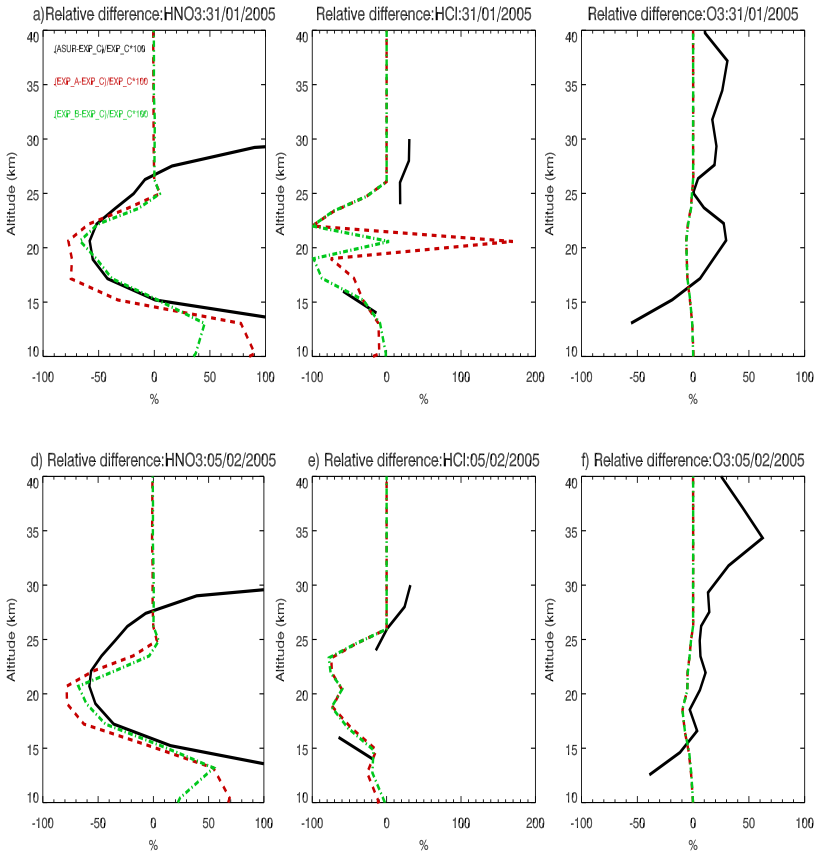

Fig. 3. The relative difference (%) of HNO_3, HCl and O_3 between ASUR measurements and SLIMCAT full chemistry simulations using the equilibrium (EXP_A) and DLAPSE (EXP_B) PSC schemes with respect to the SLIMCAT simulation without denitrification (EXP_C) for (top) 31 January and (bottom) 5 February 2005.

ACPD
11, 3857–3884, 2011

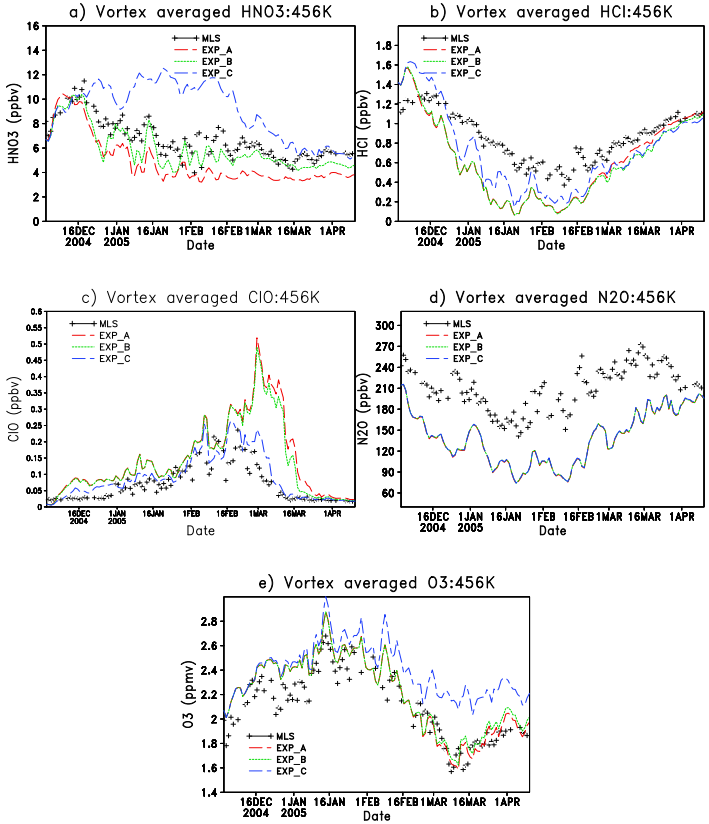

Fig. 4. Time evolution of HNO_3, HCl, ClO, N_2O and O_3 from MLS measurements and SLIMCAT simulations using the equilibrium (EXP_A) and DLAPSE (EXP_B) PSC schemes as well as the simulation without denitrification (EXP_C) at 456 K (~17 km).

ACPD
11, 3857–3884, 2011

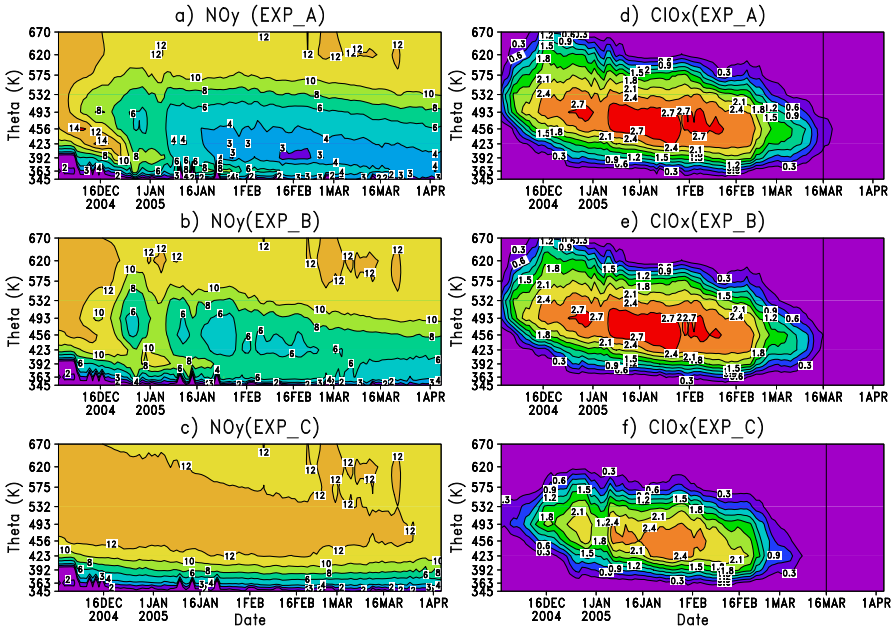

Fig. 5. Vortex-averaged NO_y and ClO_x (ppbv) as a function of time and potential temperature for SLIMCAT simulations using the equilibrium (EXP_A) and DLAPSE (EXP_B) PSC schemes and the simulation without denitrification (EXP_C) for Arctic winter/spring 2004/05.

ACPD
11, 3857–3884, 2011

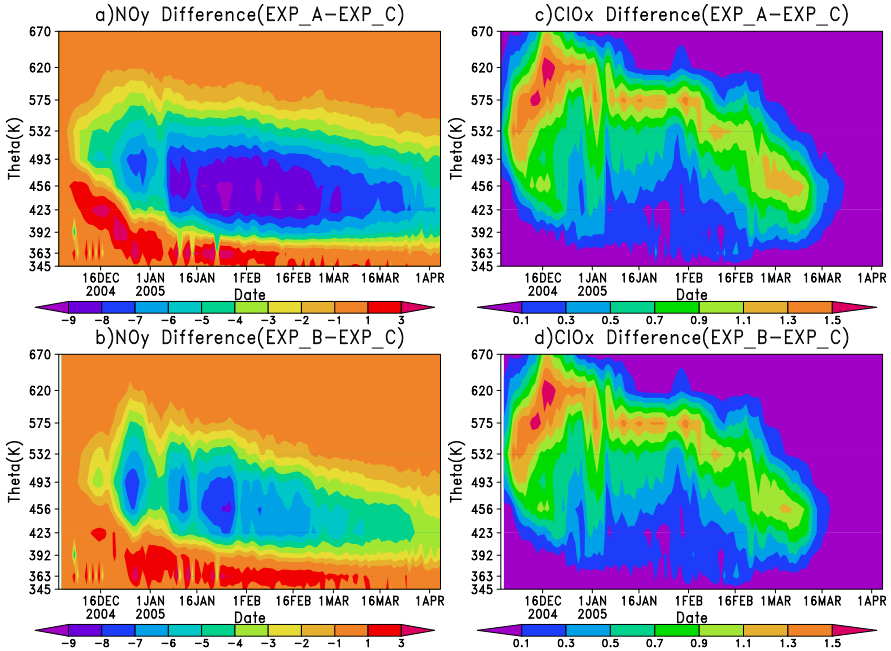

Fig. 6. Difference in vortex-averaged NO_y and ClO_x (ppbv) as a function of time and potential temperature for SLIMCAT full chemistry simulations using the equilibrium (EXP_A) and DLAPSE (EXP_B) PSC schemes with respect to the SLIMCAT simulation without denitrification (EXP_C) for Arctic winter/spring 2004/05.

ACPD
11, 3857–3884, 2011

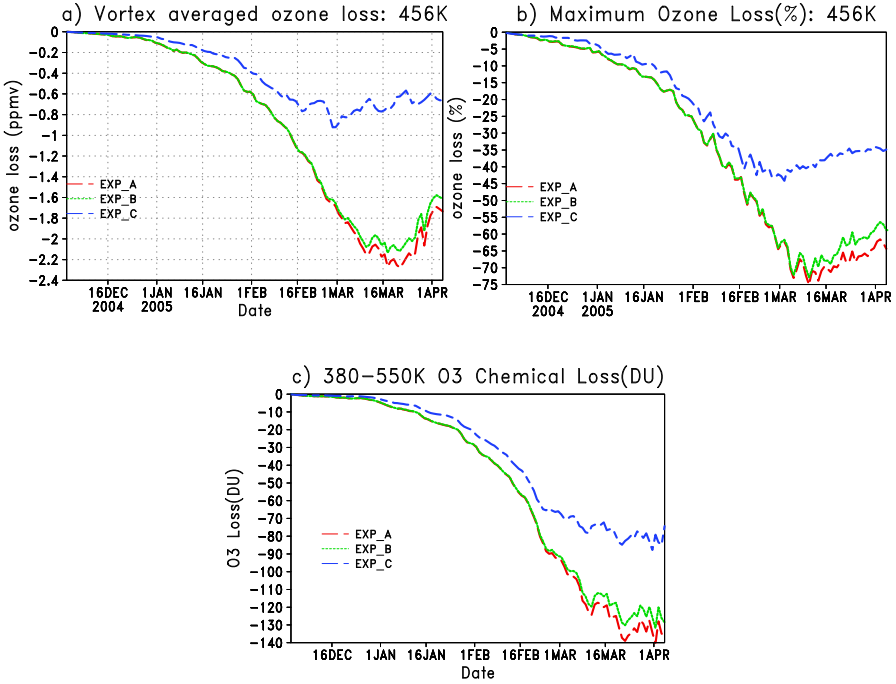

Fig. 7. Time series of **(a)** vortex-averaged ozone loss, **(b)** maximum local ozone loss at 456 K (~17 km) and **(c)** partial column ozone loss between 380–550 K (~13–25 km) from simulations using the two different PSC schemes (equilibrium and DLAPSE) and without denitrification for Arctic winter/spring 2004/05.

ACPD
11, 3857–3884, 2011

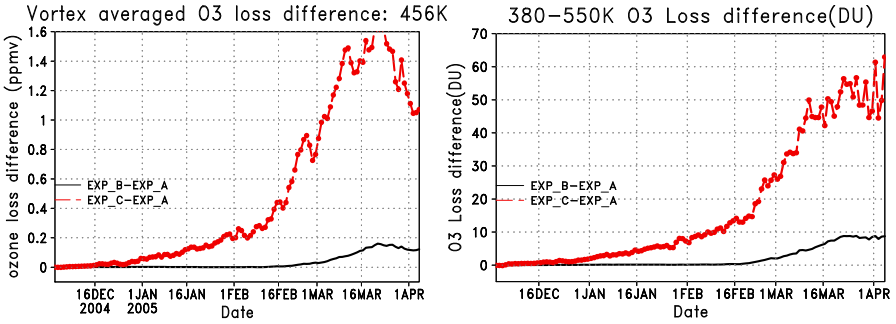

Fig. 8. Time series of differences in **(a)** vortex-averaged ozone loss ozone loss at 456 K (~17 km), **(b)** partial column ozone loss between 380–550 K (~13–25 km) between model sensitivity experiments (EXP_B, EXP_C) and standard SLIMCAT simulation (EXP_A) for Arctic winter/spring 2004/05.

ACPD
11, 3857–3884, 2011